

Beam Dynamics and Vacuum System



Jaeyu Lee & Taekyun Ha*
(PAL, POSTECH, Korea)

2022 Oct 13

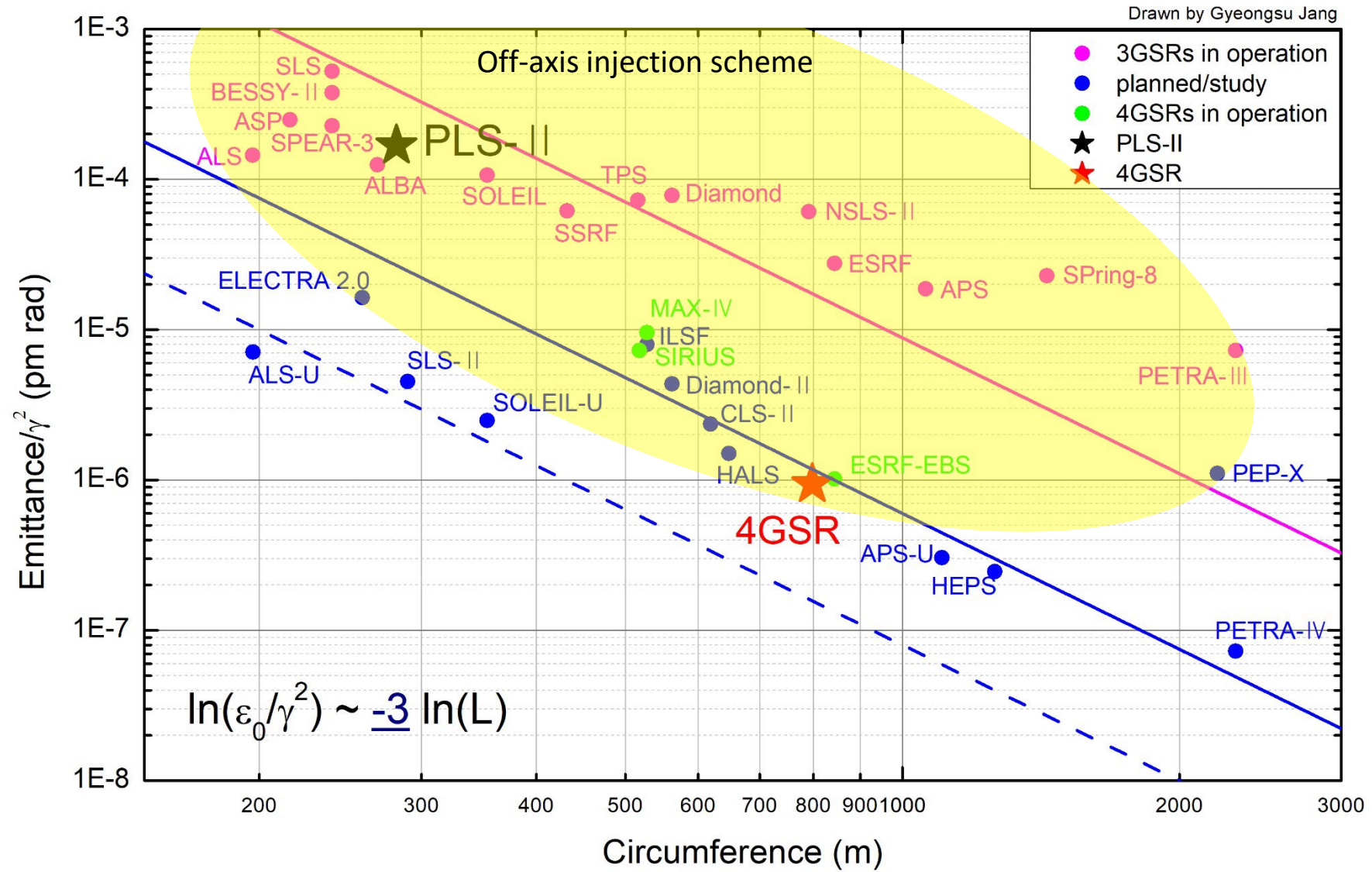


Beam Dynamics



4GSR in worldwide storage rings

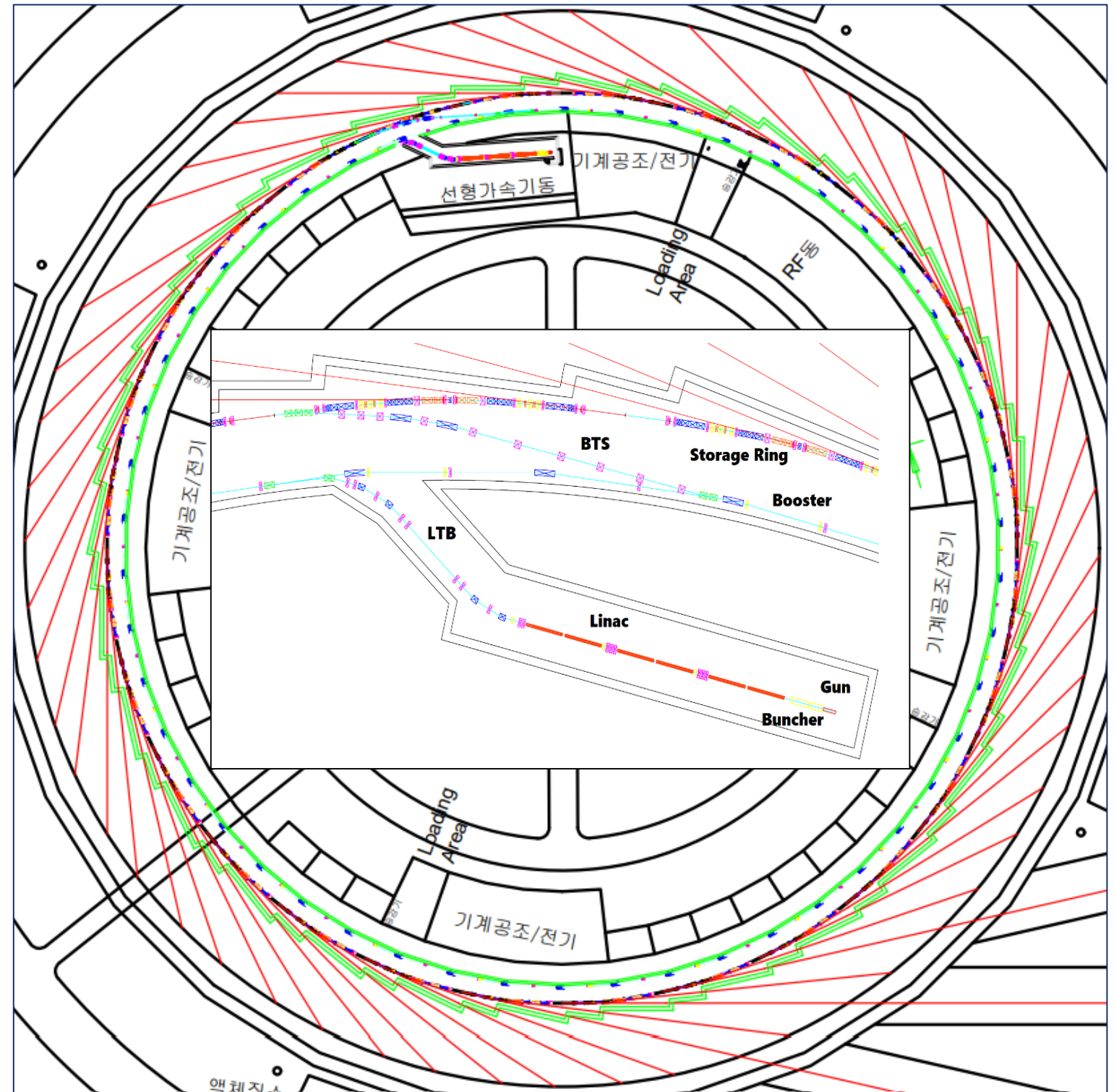
Figure 1.



CDR: Overview of 4GSR

Parameter	Units	PLS-II	4GSR
Electron energy	GeV	3	4
Horiz. Emittance	pm	5800	58 (RB: 39)
Vert. Emittance	pm	~ 58	~ 5.8 (RB: 39)
Bunch length (rms)	ps	20	13 (50 with HC)
Circumference	m	280	800
Harmonic #		470	1332
RF frequency	MHz	500	500
Beam stability @ ID (x/y)	μm	< 4 / 2	< 2.5 / 0.45
Injection mode		Top-up	Top-up

Figure 2.



Lattice design & Nonlinear

❖ Liner lattice

1. ESRF-EBS type
 - Dispersion bump w/sextupoles.
 - Longitudinal gradient dipoles.
 - Phase advance of $\Delta\phi_x \sim 3\pi$ and $\Delta\phi_y \sim \pi$ between corresponding sextupole
2. APS-U type: Reverse bends in Q4, Q5, and Q8.
3. **4GSR: 6.5 m straight section and 2 T center-bend ($E_c=21$ keV)**

❖ Nonlinear lattice

1. 2-cell modulation : different sextupole's strength in 1st and 2nd cells
2. 2 sextupoles for chromaticity correction and 10 sextupoles for nonlinear dynamics in 2-cell
3. MOGA optimization.
4. Enough on-momentum DA.
5. Relatively small off-momentum DA.
 - => No octupole magnet used yet (On study).
 - => Large energy dependent tune shift.
 - => But still enough lifetime.

Figure 3.

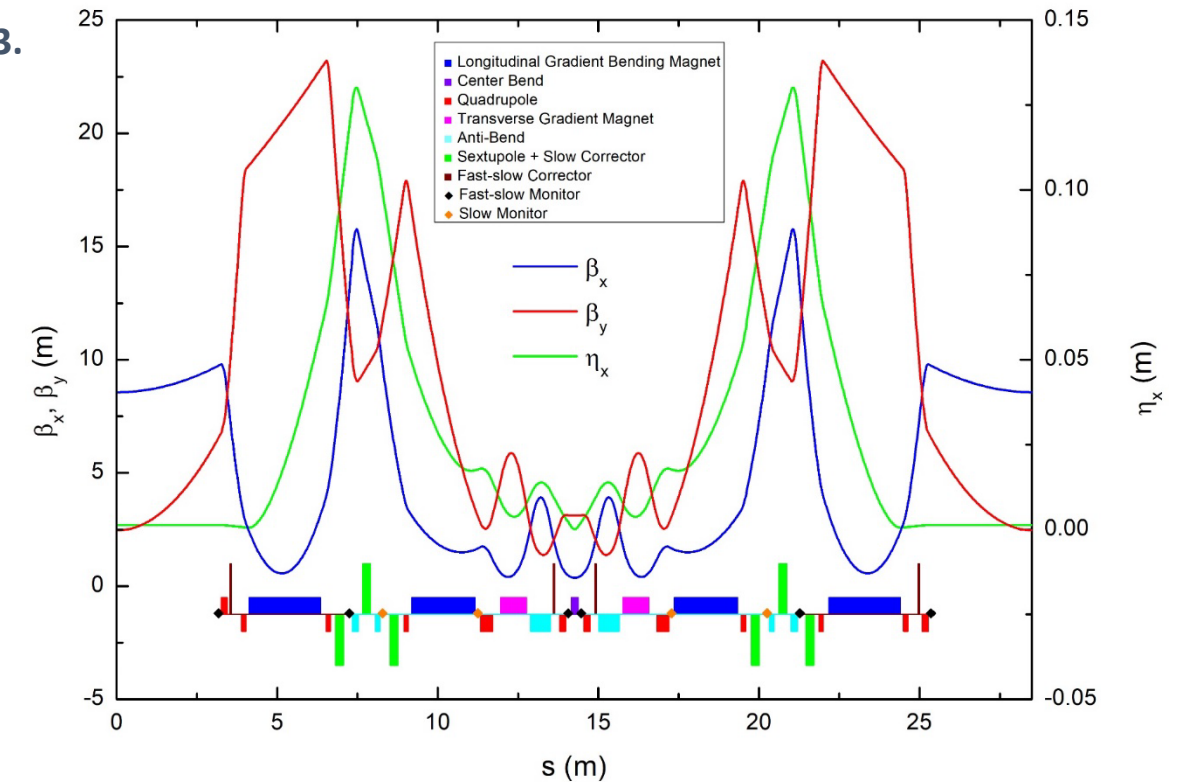
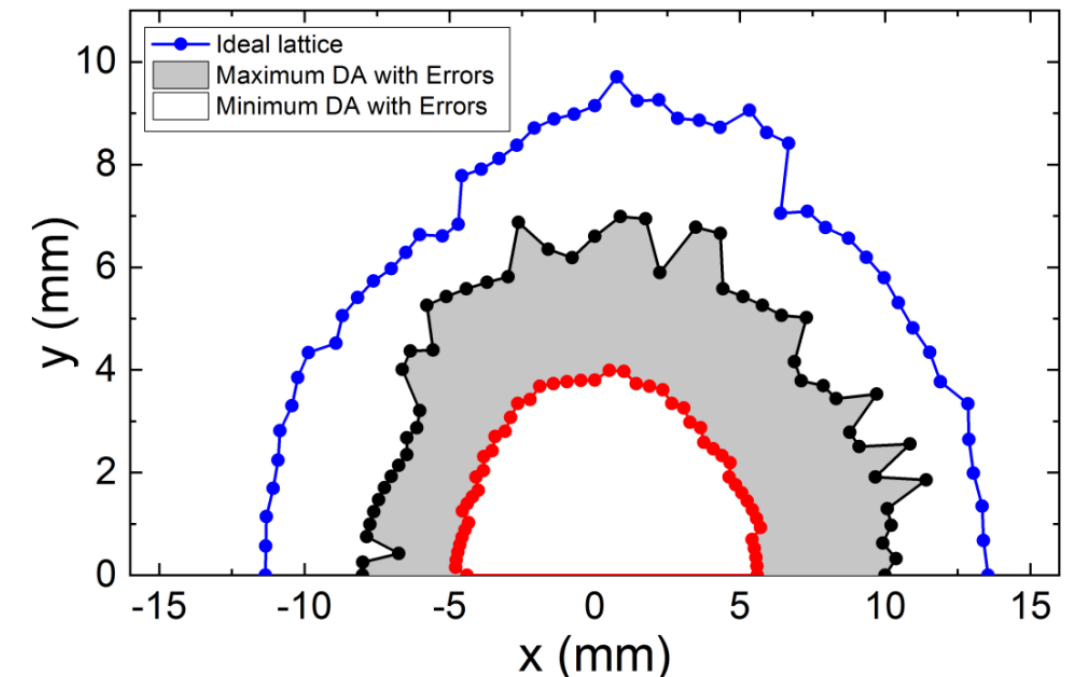


Figure 4.



Lattice finalization for TDR (in progress)

❖ Lattice - Magnet - Vacuum iteration.

- Beam dynamics solution from simulation.
- Magnet design satisfying the required field.
- Vacuum chamber design fitting the required space.
- Vacuum chamber design satisfying the required vacuum.

Figure 5.

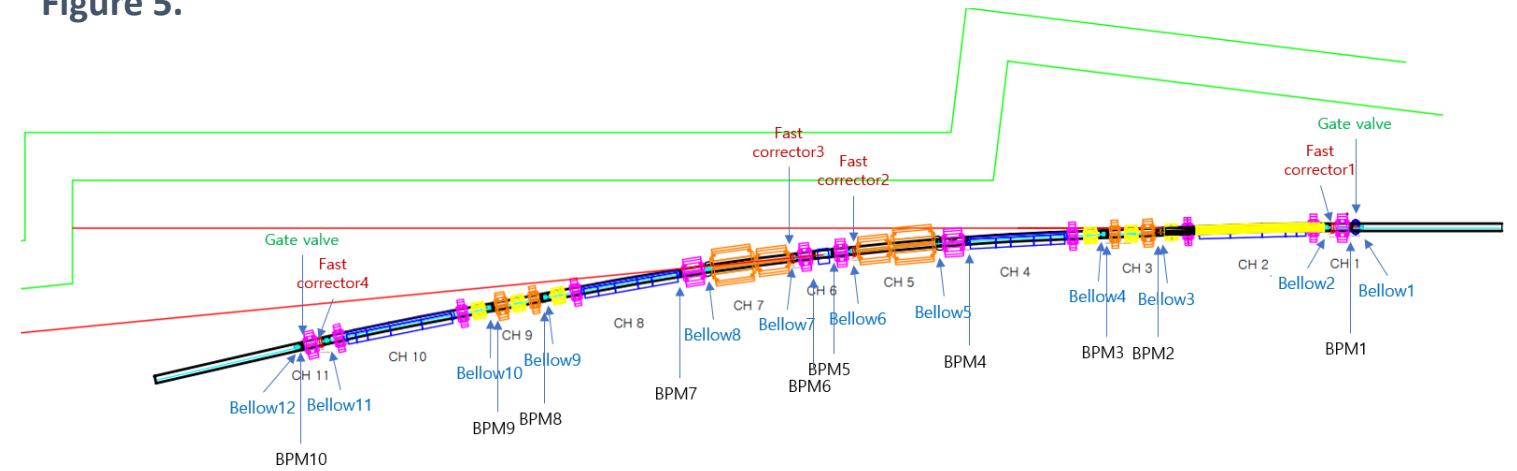
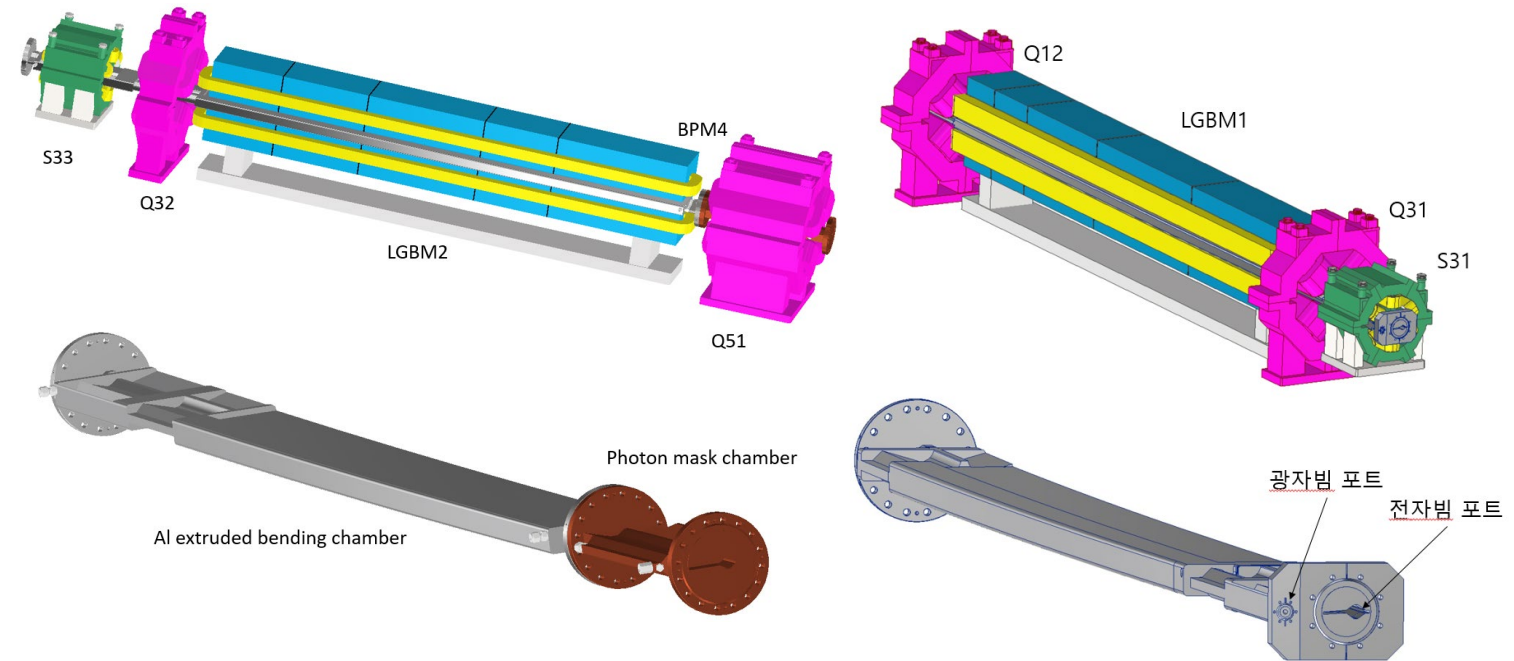


Figure 6.



Linear Accelerator

❖ 200 MeV injector to Booster.

- Change from CDR: Photo-cathode gun.
- The base design adapted successful PAL-XFEL experience.
(with XFEL manpower)

❖ Main components

- Photo-cathode and UV laser.
- Acceleration tube and waveguide system.
- S-band LLRF and SSA
- Klystrons and pulse powers

Figure 9.

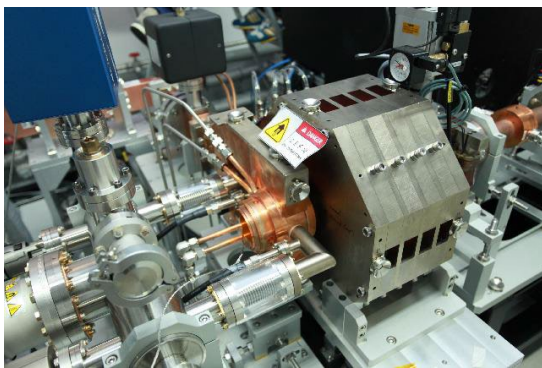


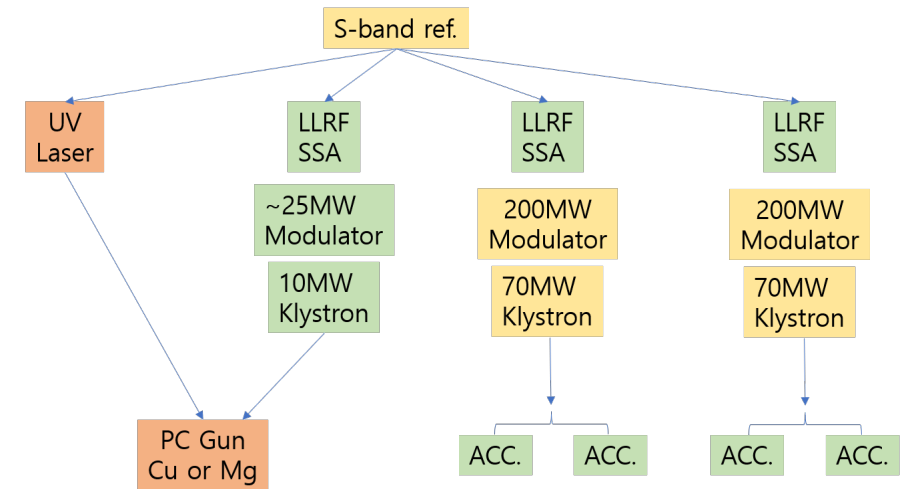
Figure 10.



Figure 7.



Figure 8.

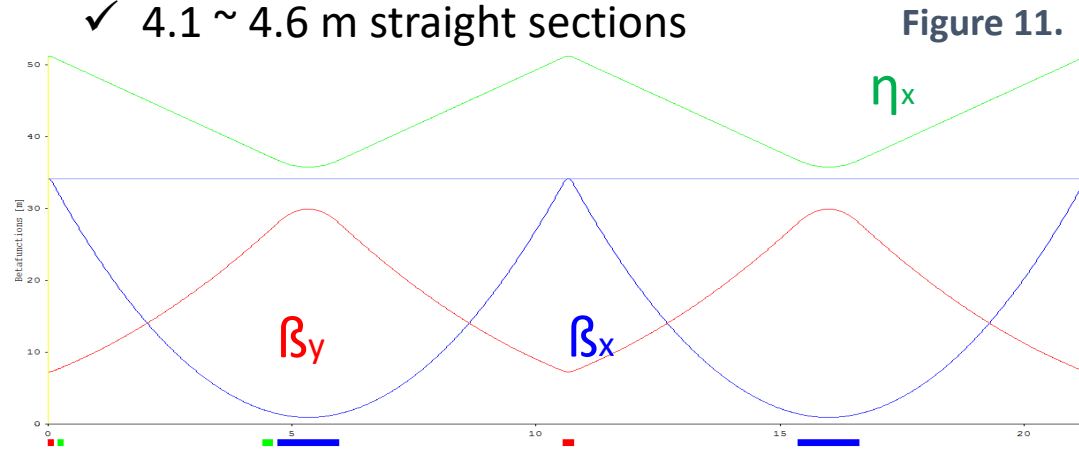


	Single-bunch mode	Multi-bunch mode
Beam energy	200 MeV	200 MeV
	0.01 ~ 1 nC	1 ~ 3 nC
Emittance	< 10 nm	< 10nm
Pulse length	< 20 ps	200 ns (100 bunches)
Repetition rate	2 Hz	2 Hz

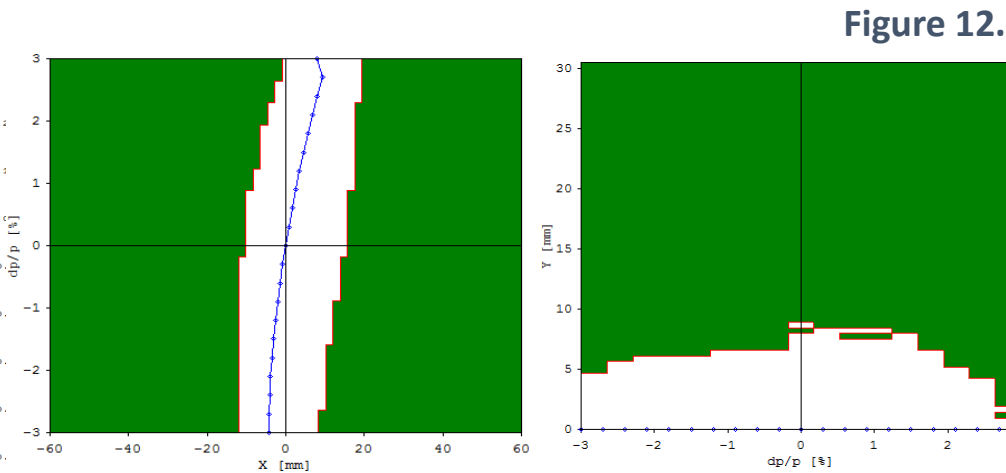
Booster

• **Linear Lattice**

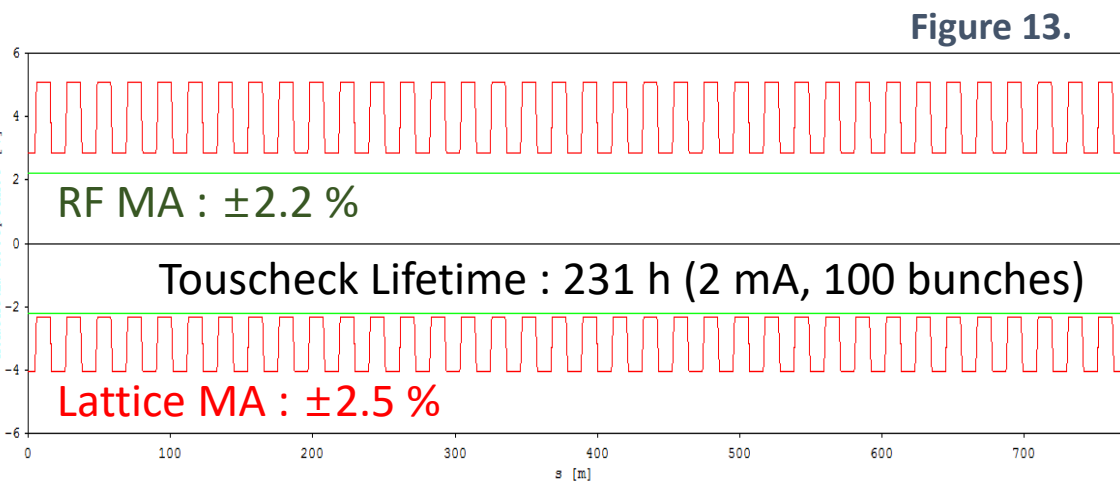
- ✓ 21.324 m FODOFODO cell X 36
- ✓ 4.1 ~ 4.6 m straight sections



• **Dynamic Aperture vs dp/p ($\pm 3\%$)**



• **Momentum Aperture**



• **Beam Stay Clear**

$$A_x = 3\sqrt{\beta_x \epsilon_x + (\eta_x \sigma_\delta)^2} + x_{COD} + x_{\beta_{osc}} + \eta_x \delta_{osc} = 9.9 \text{ mm at Quadrupole}$$

$$A_y = 3\sqrt{\beta_y \epsilon_y} + y_{COD} + y_{\beta_{osc}} = 4.8 \text{ mm at Dipole}$$

⇒ Hor. 11 mm Ver. 6 mm radius elliptical chamber

Parameter	Value	Unit
Injection energy	0.2	GeV
Extraction energy	4	GeV
Circumference	767.664	m
Beam current	< 2	mA
Revolution time	2.56	us
Cycling frequency	2	Hz
Betatron tune (H/V)	30.16 / 8.28	
Momentum compaction	0.000241	
Natural chromaticity (H/V)	-69.7 / -21.5	
Natural emittance	1.483	nm
Natural energy spread	0.094%	
Damping time (H/V/L)	11.5 / 13.1 / 7.0	ms
RF frequency	499.8728	MHz
Rad. Loss per turn	1.483	MeV
Gap voltage	3	MV
Harmonic number	1280	
Synchrotron tune	2190	Hz
Rms Bunch length	4.9	mm

Magnet Type	Number	Length(m)	Max. Field
Dipole (Combined Function, QD)	72	1.262	0.9226 T -2.26 T/m
Quadrupole (QF)	72	0.2	22.6 T/m
Sextupole (SF, SD)	36, 36	0.1, 0.2	225.1, -396.1 T/m ²
Total	216		

RF system in storage ring

❖ Normal conducting cavity.

- Change from CDR: SRF -> NC .
- No cryo-genic system and cryo-module.

❖ 400 mA beam current.

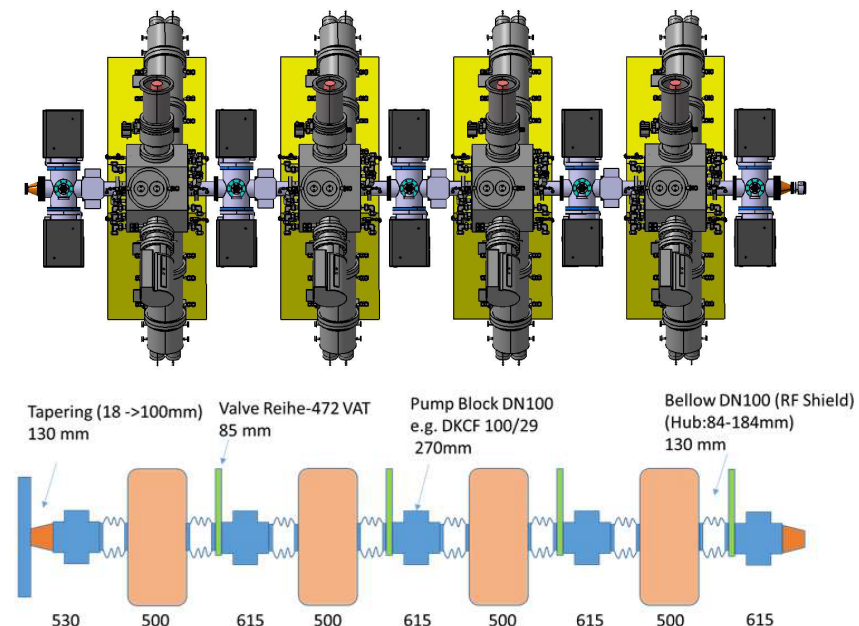
- HOM damper (EU) NC cavity.
- Longitudinal bunch by bunch feedback system.
- Transverse bunch by bunch feedback system.

❖ Higher Harmonic cavity

- To increase beam lifetime (3 hr. -> 10 hr.)
- To reduce heat load (by increasing bunch length)

Parameter	Unit	Values	Remark
Total accelerating voltage	MV	3.5	
Number of cavity	-	10	
Coupling beta	-	~5.5	for minimum reflect power @ 400 mA
Each required accelerating voltage	MV/unit	0.35	
Wall loss power per cavity	kW/unit	18.01	
Beam loading power per cavity	kW/unit	74.00	62.40
Power loss at HOM absorber	kW/unit	5.00	
Each required power to coupler	kW/unit	97.02	85.42
Transmission line loss per cavity	kW/unit	10.00	circulator, waveguide, etc.
Output power of HPRF	kW/unit	107.02	95.42
Rated power of HPRF	kW/unit	178.36	107.0 2 power linearity (Max. power 60~70%)
Total AC power for RF source (klystron case)	kW	4458.97	2675. 38 operation efficiency : 40 %
Total AC power for RF source (SSPA case)	kW	3963.53	2378. 12 operation efficiency : 45 %

Figure 14.



Photon beam study

❖ Photon beam characteristics.

- From source to whole beam line.
- On discussion with BL.

❖ Error and tolerance study.

- Good reference for beam line design.

❖ Heat load and cooling.

- Heat load (> 5 times)
- Benchmark study with PLS-II

(Estimation: 32 degree)

(Measurement: 29 degree)

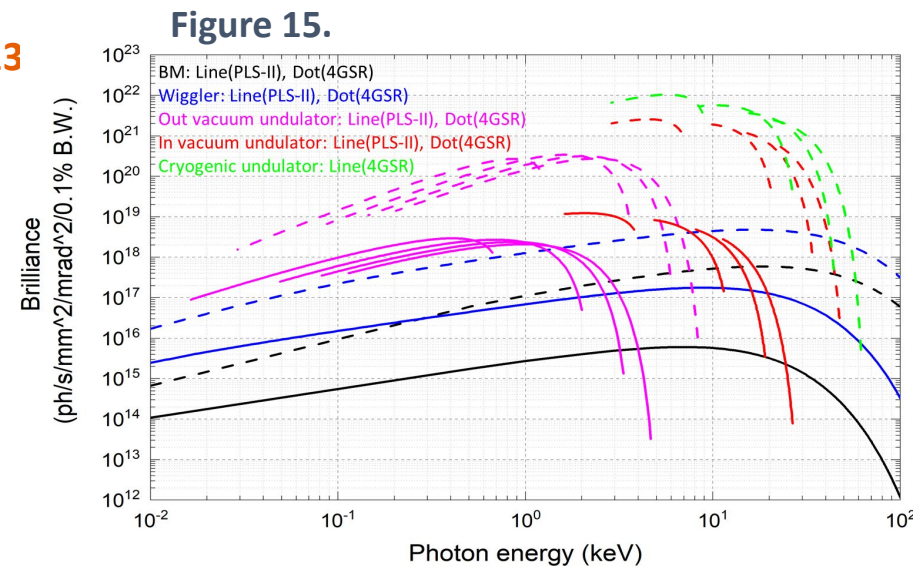


Figure 16.

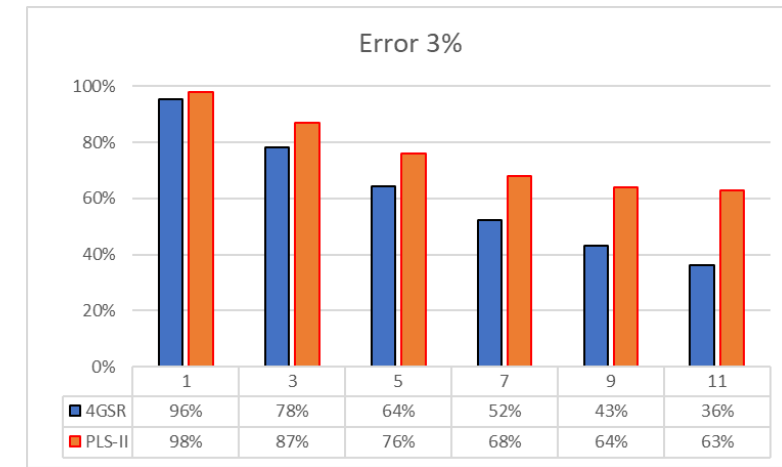


Figure 17.

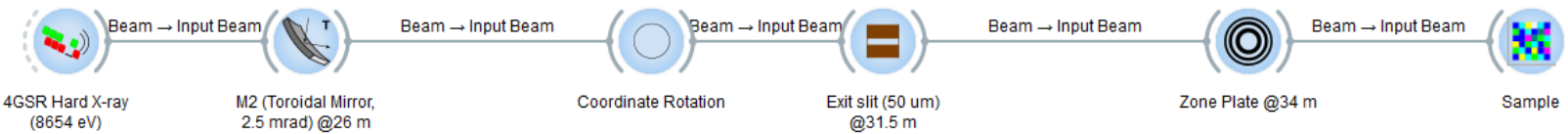
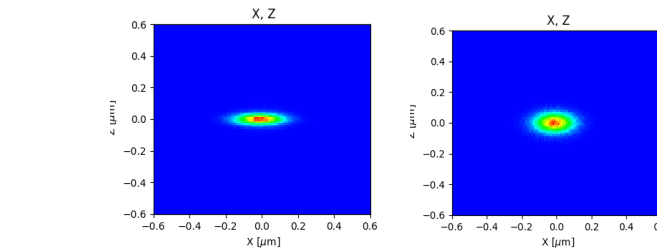
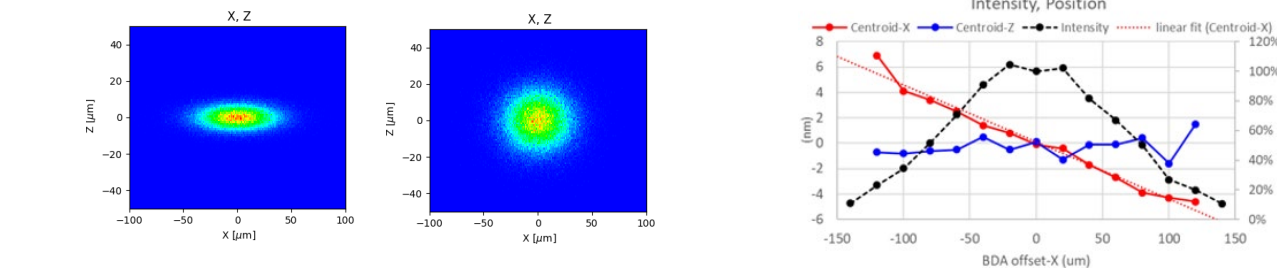
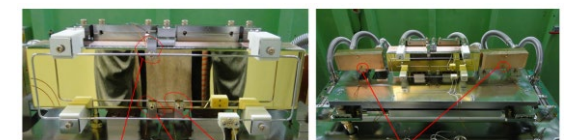
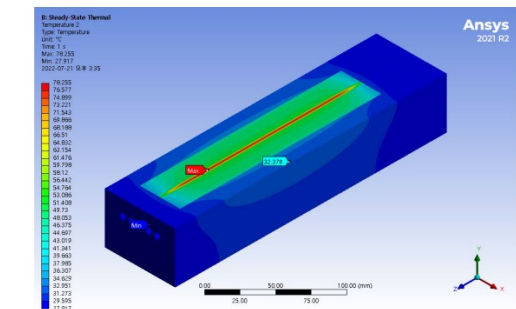
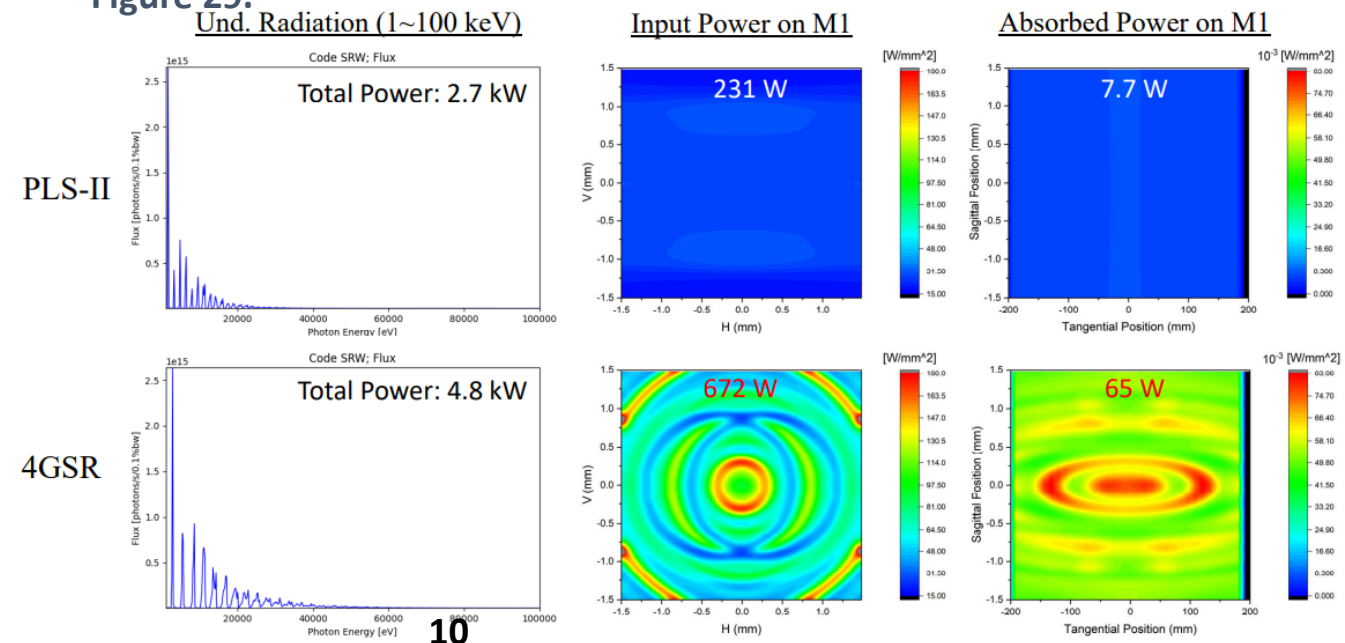


Figure 18.



➤ Max: 78 °C, Meas. Point: 32 °C

Figure 29.



Summary

❖ Korea 4th Generation Storage Ring (4GSR) has 3 design features

- The best performance in the range of 10 ~ 30 keV and capability to generate photon beam up to 100 keV.
- Considering well-demonstrated technologies for the on schedule user service with full performance.
- Synergy with PLS-II and PAL-XFEL to support full range of synchrotron radiation application.

❖ Current status of 4GSR lattice design

- 4GSR is designed with 800 m, 4 GeV, 60 pm emittance storage ring with hybrid 7BA structure.
- 4GSR has 28 cells and each cell accommodate 6.5-m-long straight section and 2 T bending source.
- 200 MeV linac with photo-cathode gun and 768 m, 1 nm emittance booster ring enable high and efficient injection.

❖ Further study

- Design iteration and fine-tune between beam–magnet–vacuum until the end of 2022
- Design of high-beta injection cell for Large DA and beta matching of ID section for high brightness
- Calculation of beam instability threshold
- Technical design report by September of 2023

Vacuum System



Vacuum system overview

1. Required average pressure is low 10^{-9} mbar for SR and 10^{-8} mbar for booster (CO equivalent).
2. Required pressure for linac is below 10^{-11} mbar for PC gun and 10^{-8} for accelerating column.
3. PSD gas in SR is pumped by distributed pill-type NEG and lumped sputter ion pumps.
4. 5° Inclined side chamber wall absorbs synchrotron radiation in SR.
5. Thermo-mechanical analysis results show that both aluminum and copper alloy are suitable for the SR vacuum chamber material.
6. Booster ring vacuum chambers are made of 1 mm-thick stainless steel and pumped with lumped Sputter ion pumps.

Figure 1. Cross section of the SR vacuum chamber

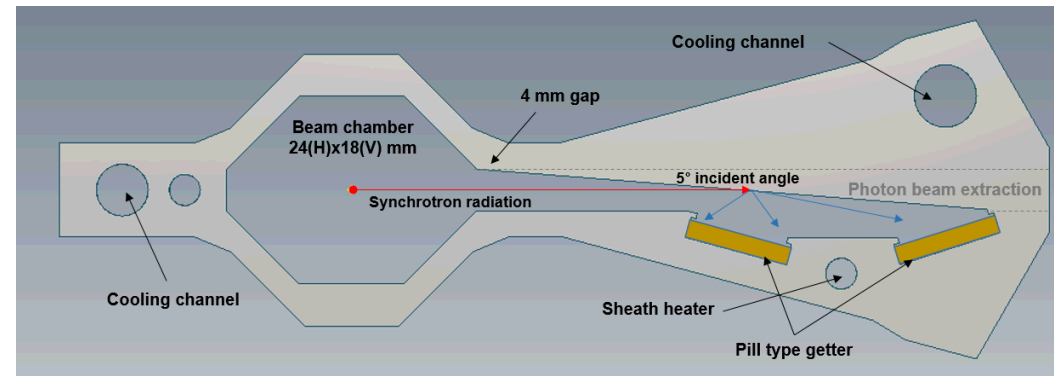


Figure 2. Beam stay clear

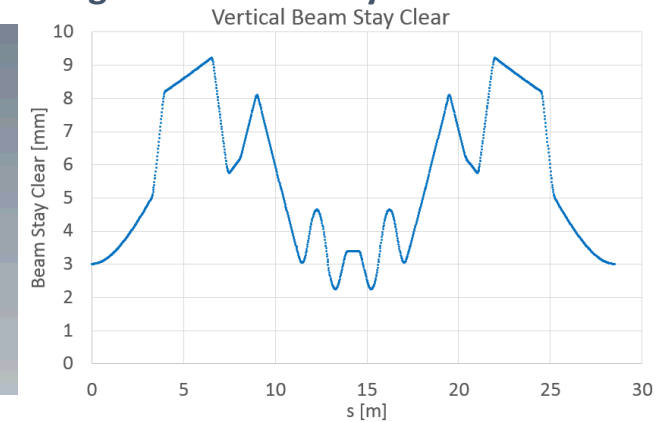
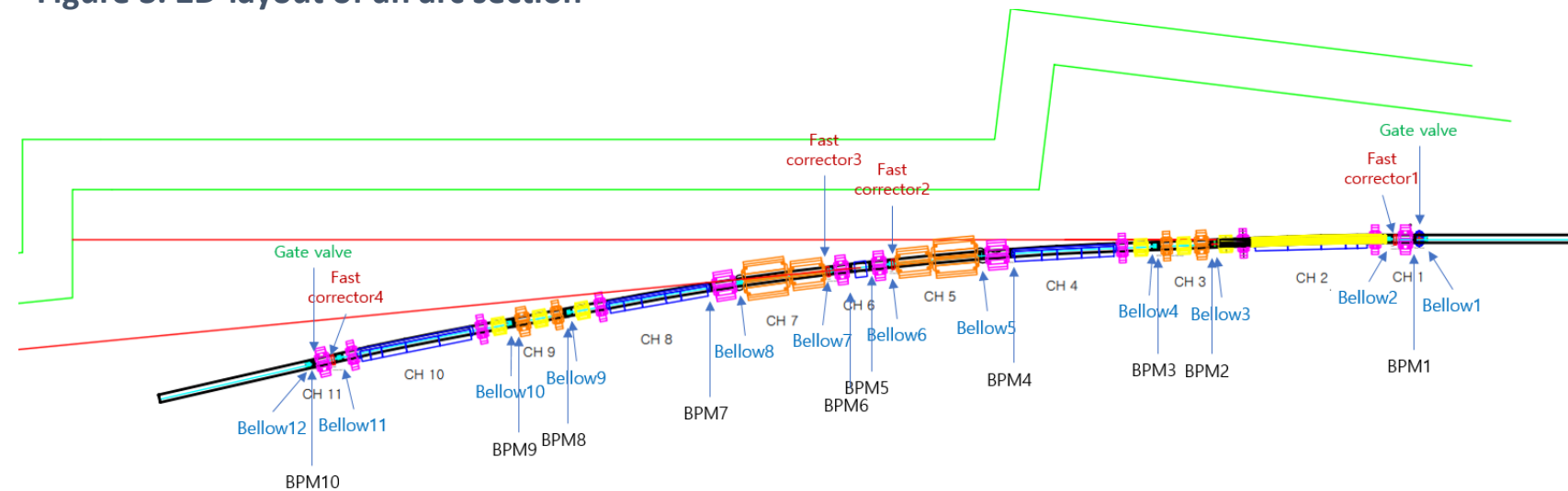


Figure 3. 2D-layout of an arc section



SR vacuum chamber

❖ Main feature

- Beam chamber cross section is octagon shape (24 mm (H) x 18 mm (V)) except for center bend.
- Vertical aperture of the center bend chamber is 10 mm.
- Eight RF-bellows are used for installation and to reduce stress.
- Two gate valves are located at the end of the arc section.
- Seven sputter ion pumps are installed for noble gas pumping.
- The clearance between the vacuum chamber and the magnets is larger than 0.6 mm.

Figure 4. Clearance between vacuum chamber and magnet

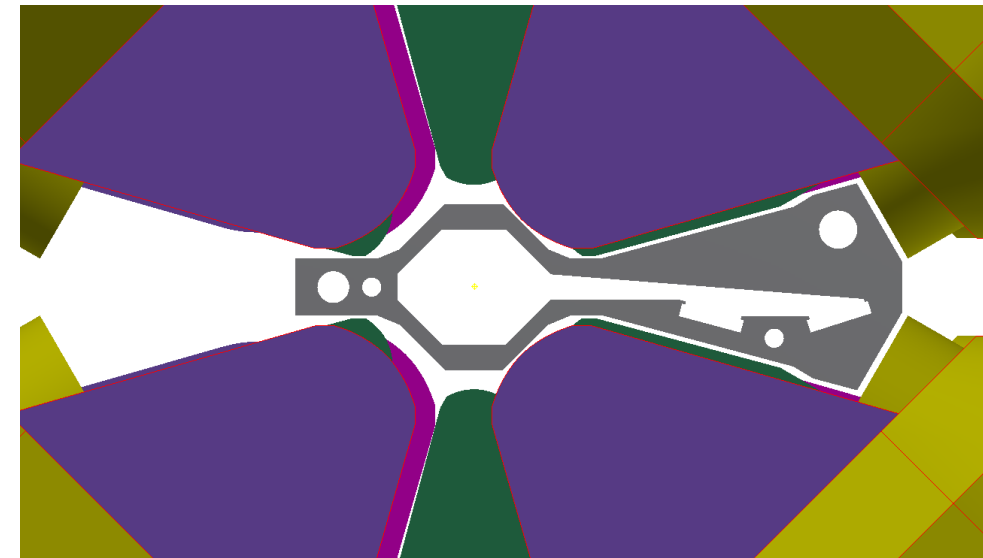
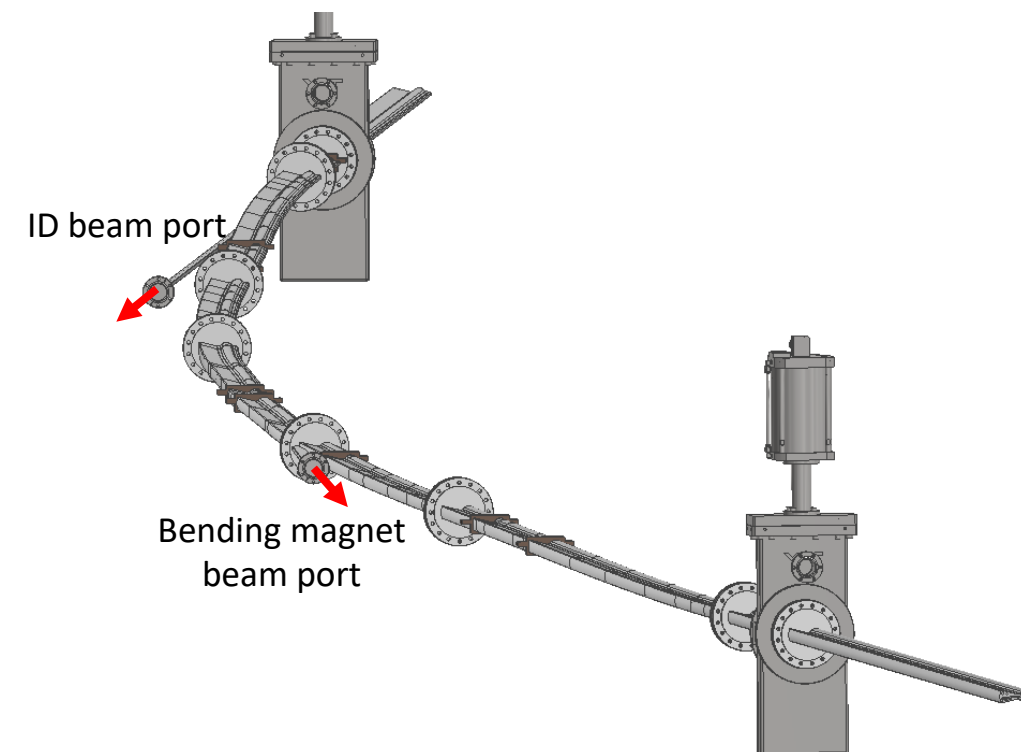


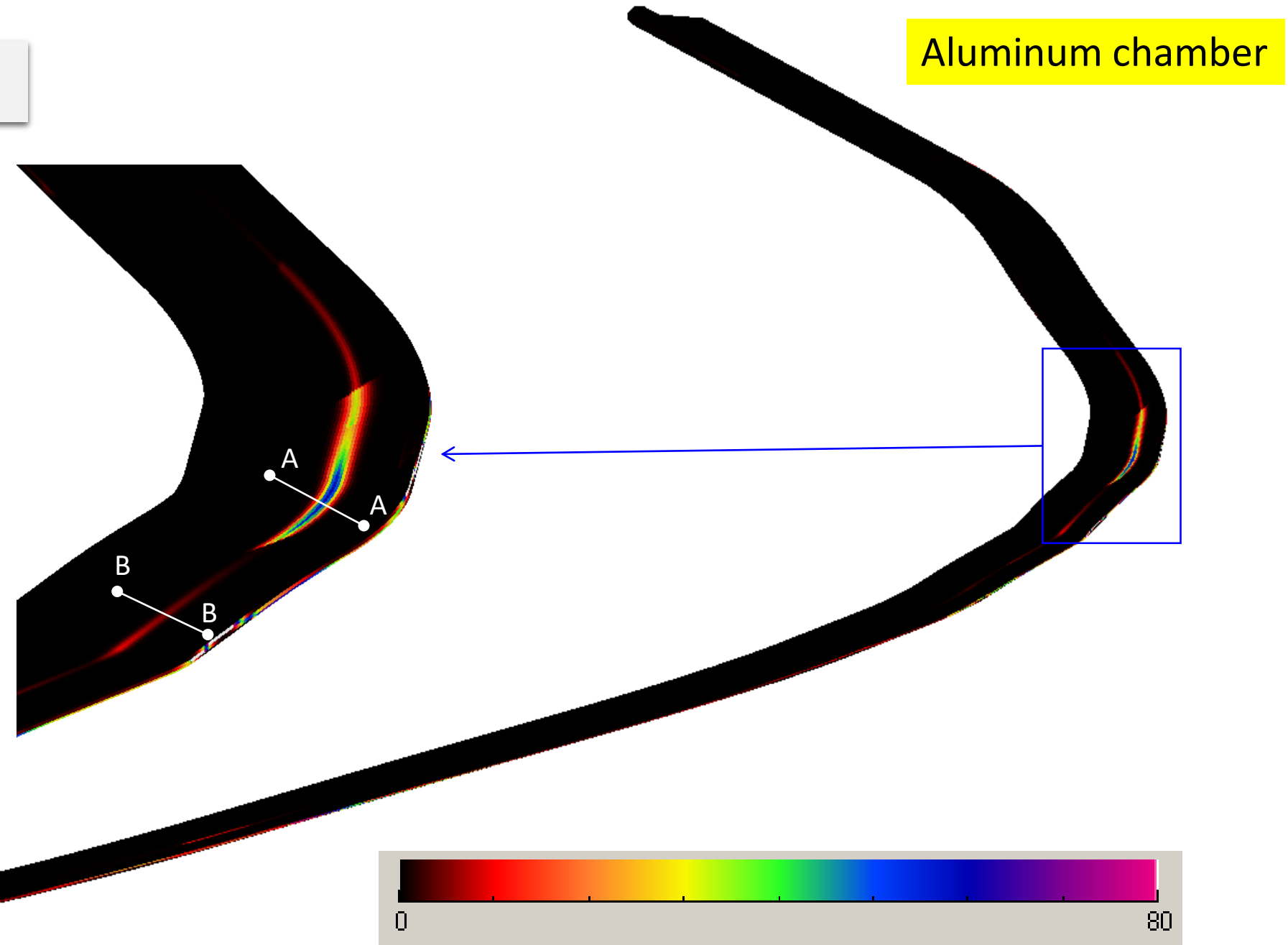
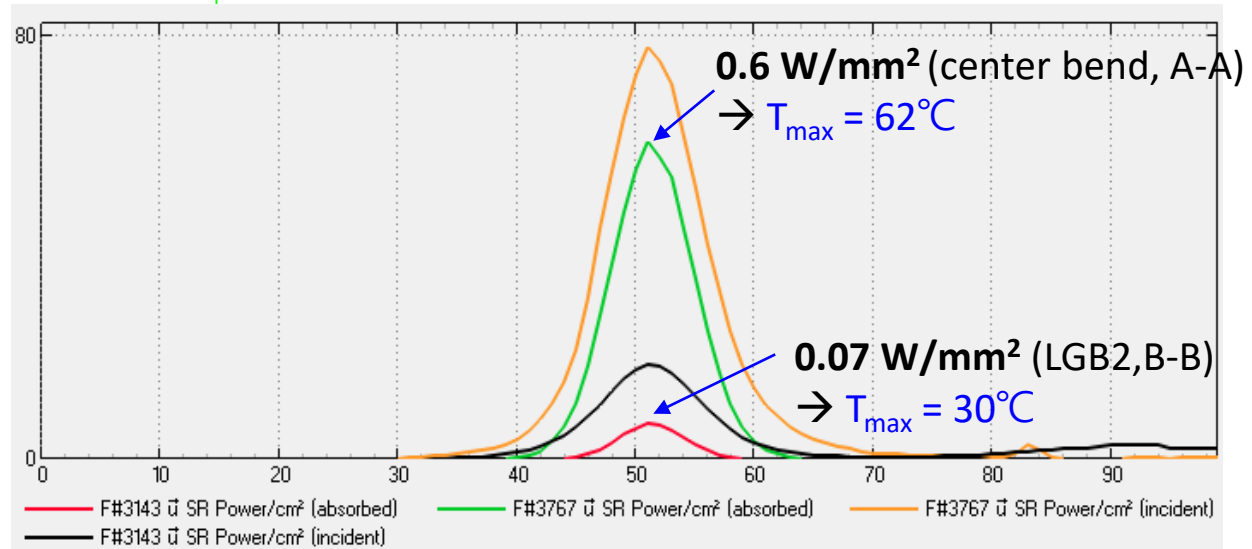
Figure 5. Vacuum chamber of an arc section



SR heat load (Synrad+)

Figure 6. SR power on the side chamber wall

- from C-bend (line AA): — incident, — absorbed
- from LGB2 (line BB): — incident, — absorbed



Thermomechanical analysis

❖ Handling of SR heat load and selection of chamber material

- Most intense thermal load is 0.77 W/mm² from the center bend.
- Thermal analysis results show that both aluminum and Cu alloy can be used for the vacuum chamber material.
 - Aluminum chamber can be fabricated by extrusion, bending and welding.
 - Cu alloy chamber can be fabricated by machining of two pieces (top and bottom) and welding.
- Temperature of the sharp edge at a beam exit branch is 68°C (endurable).

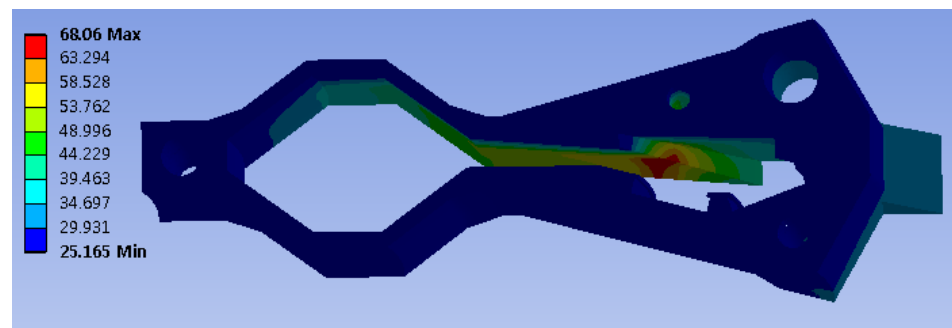


Figure 7. Temperature of the chamber wall at a beam exit

❖ Heat load from Center Bends

	B	Bend angle	Total power	Source distance	Inc_angle (H)	Inc_angle (V)	Foot print V-height	Thermal load
Center bend	1.96 T	1.6°	6 kW	2.25 m	2.35°	5°	0.44 mm	0.77 W/mm ²

❖ Results

Material	T _{max} (chamber)	T _{max} (Water channel)	σ _{max}	σ _{yield} (Cold worked)
Al6061T6	73°C	46°C	5.4 MPa	214 MPa
OFC Cu (C10100)	58°C	40°C	9 MPa	120 MPa
CuCrZr (C18150)	60°C	41°C	11 MPa	210 MPa

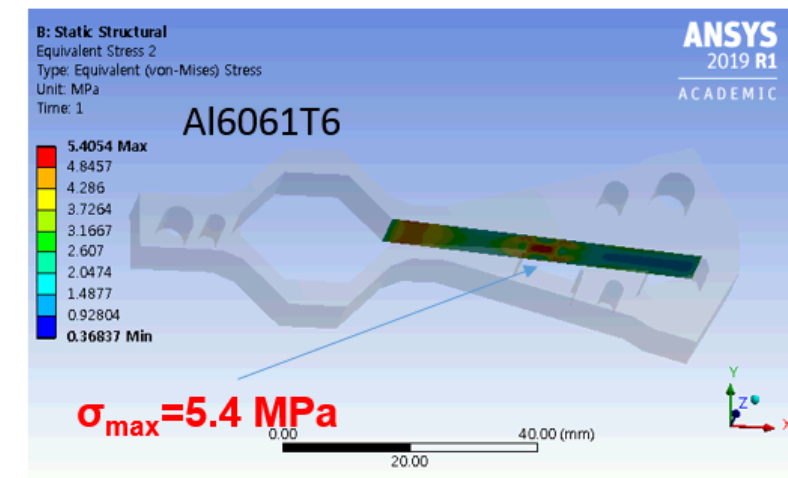
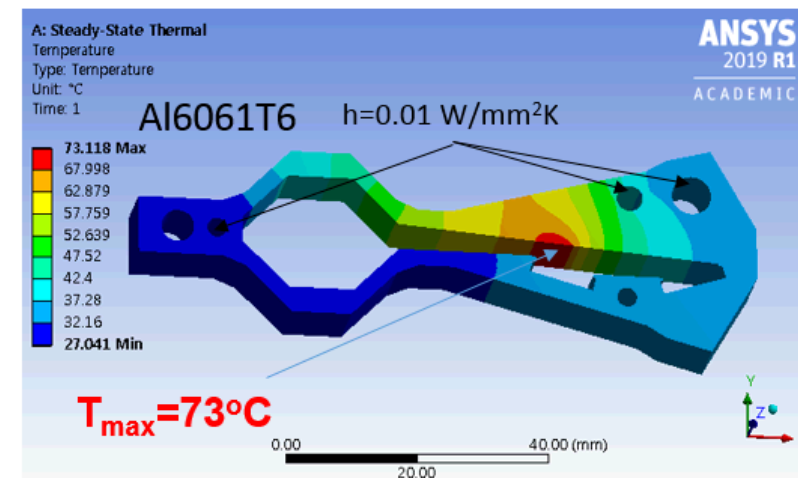


Figure 8. Thermo-mechanical analysis of the chamber wall (SR from the center bend)

Dynamic pressure calculation

❖ Photon stimulated desorption

- Total SR flux is 4.9×10^{19} ph/sec by Synrad+ simulation
- PSD yield of 1×10^{-6} /ph is used with assumption of 1000 Ah beam dose.
- Total photon stimulated desorption calculated by Synrad is 3.8×10^{-6} mbar l/s.

Figure 9. Synrad+ simulation (photon flux)

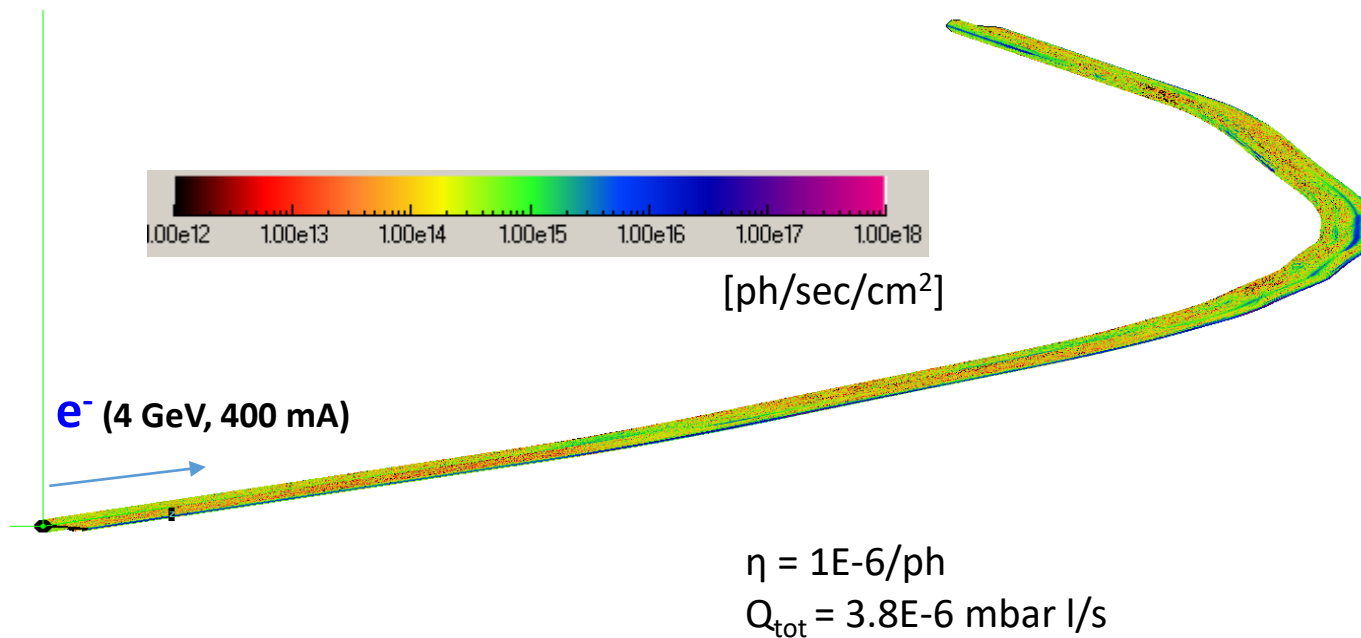
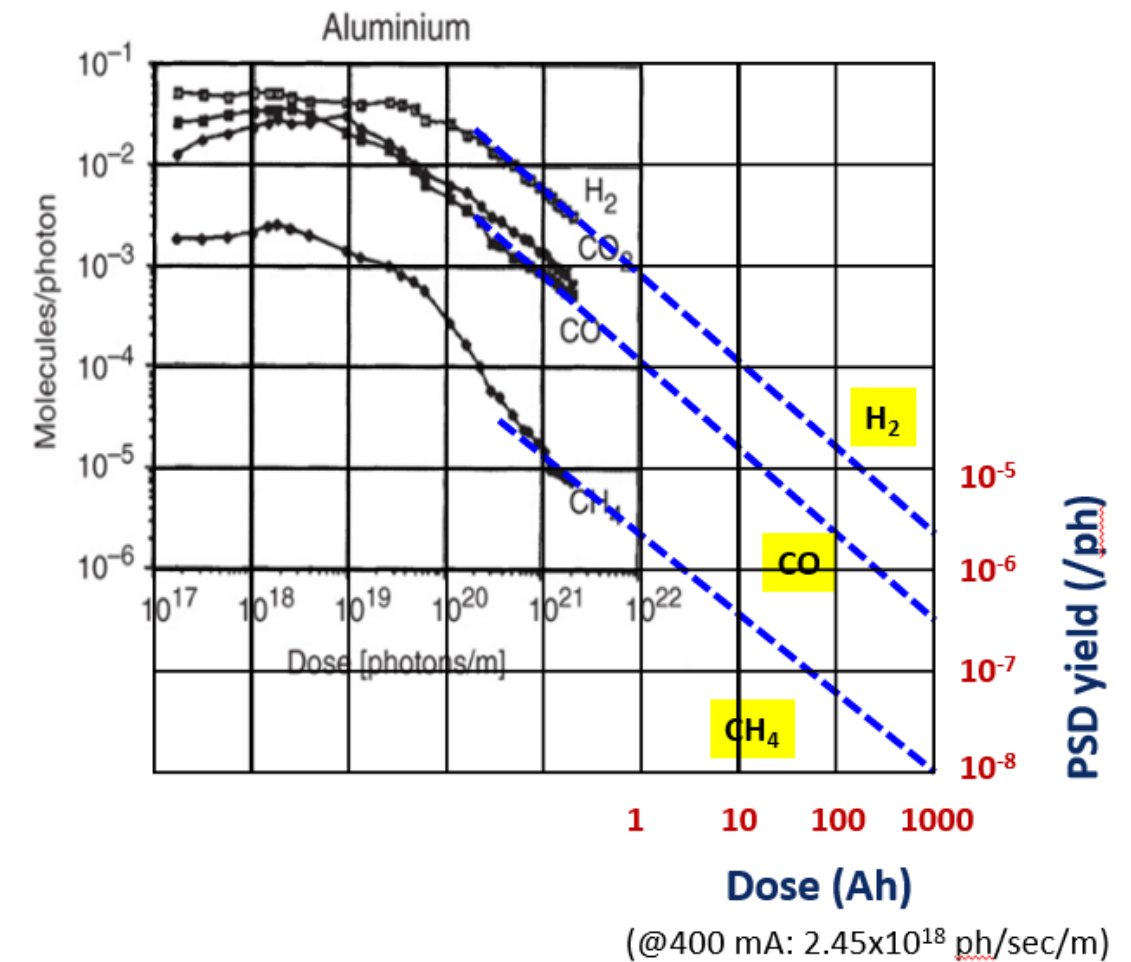


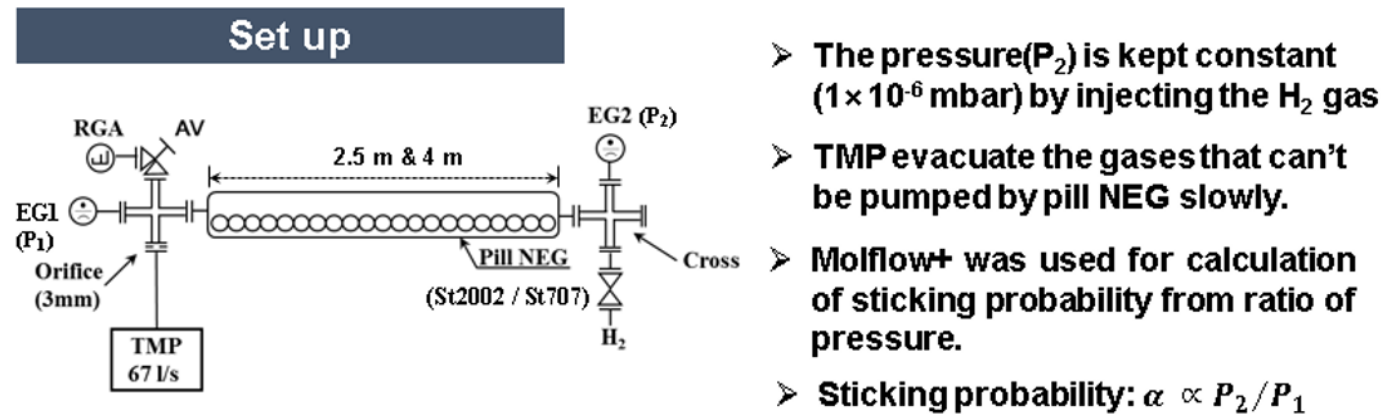
Figure 10. PSD yield of Aluminium



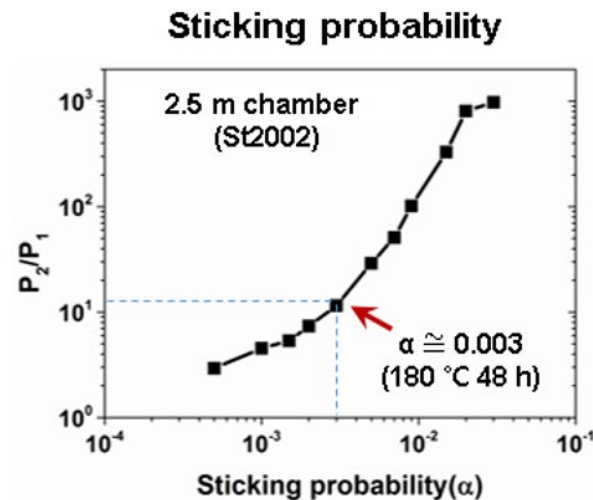
“A. Mathewson, AIP Conf. Proc. 236 (1), 313 (1991)”

Dynamic pressure calculation

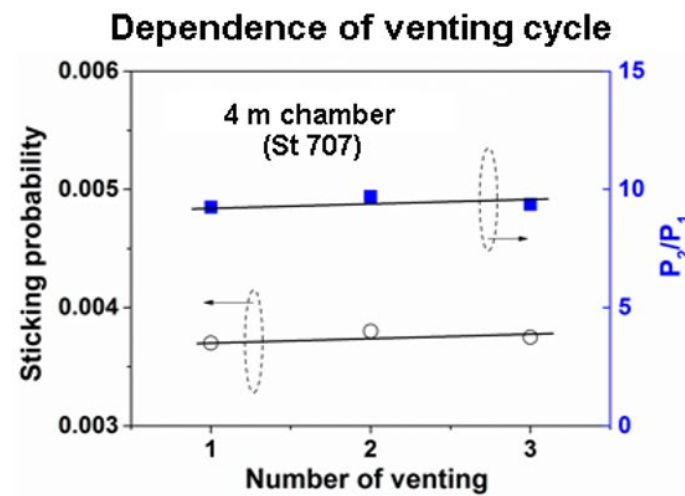
Figure 11. Pumping speed measurement for NEG pump



Results of H_2 sorption



➤ Pill NEG have a value of sticking probability about 0.003 \rightarrow 1/5 of a NEG coated chamber roughly.



➤ Sticking probability is substantially constant after three additional venting.

Figure 12. 2D-layout of an arc section

Type	NEG film (~1 μ m)	Pill-type NEG	Note
Facture	Sintering	Compressing	
Activation	200°C, 1 d	180°C, 1 ~ 2 d	
Pumping speed per length	-	Low (< 1/10)	Surf. Area \downarrow
Sticking probability (α)	0.015 (200°C, 24 h)	0.003 ~ 0.0037 (180°C, 48 h)	
α (after two additional venting)	0.015 \rightarrow 0.008	Substantially constant	
Capacity (H_2)	-	1000 \times	Thickness \uparrow
Disadvantages	Aging after venting	Particle	

Dynamic pressure calculation

❖ H₂ pressure distribution (Molflow+)

- 0.0035 is used for the sticking coefficient of pill-type NEG.
- Average pressure with only pill getter pumps is 5×10^{-9} mbar and 4×10^{-9} mbar with additional 7 sputter ion pumps.
- Wire heater is inserted into the side channel of the vacuum chamber for 180°C bake-out.

Figure 13. Molflow+ simulation

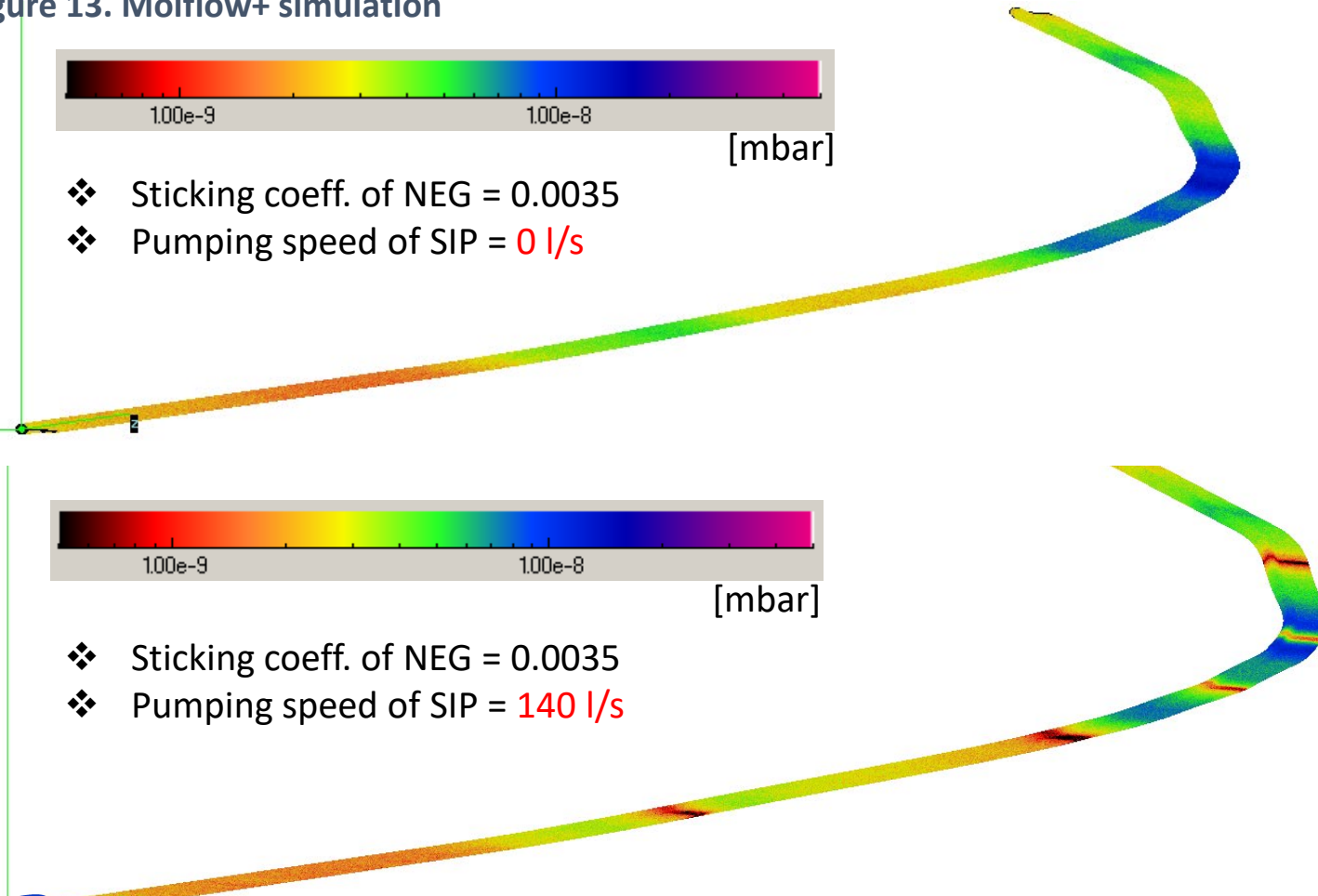
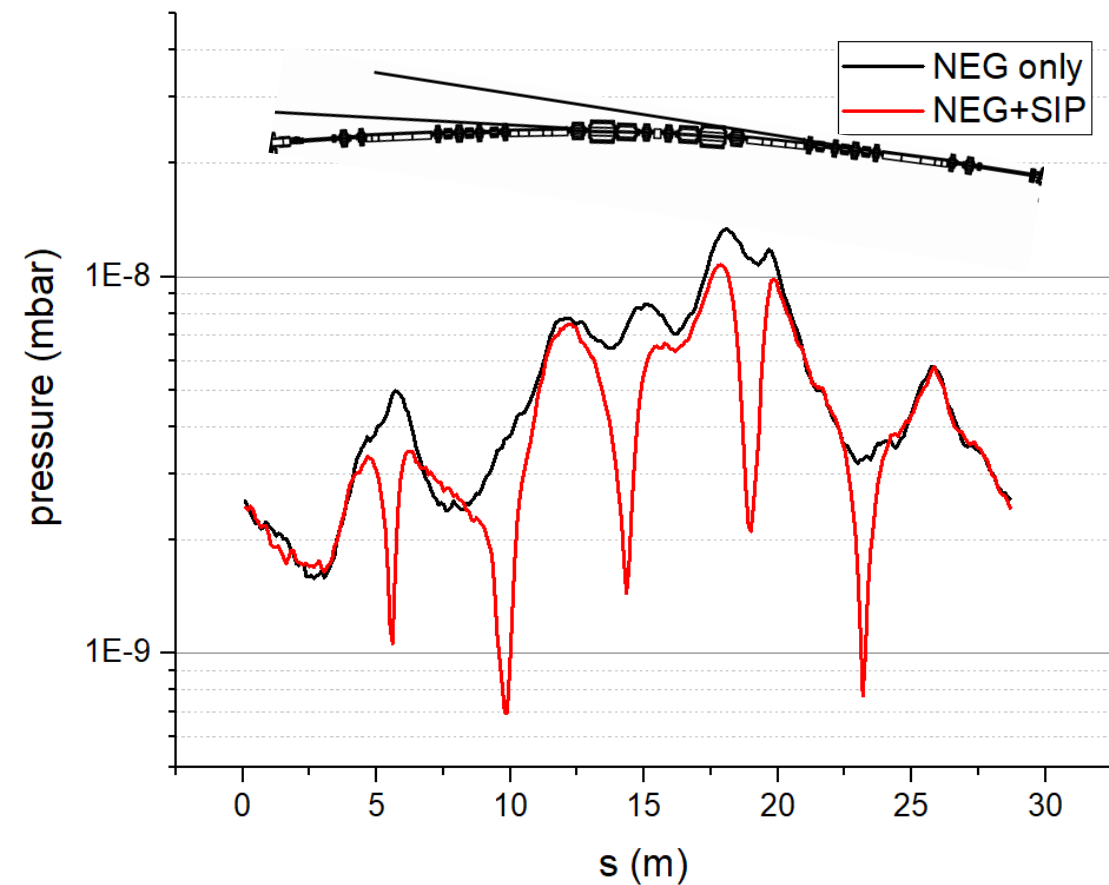


Figure 14. Pressure distribution



Prototype of SR chambers

❖ Fabrication process

1. Extrusion (A6063-T6)
2. Bending
3. Machining
4. TiC coating on the knife edge of the flange
5. Welding (flange, BPM chamber)

❖ Prototype chamber

- Making process of the vacuum chamber by local companies has been checked (no problem)
- 3D modeling of 4 bending chambers out of 11 chambers is finished
- Prototype of SR chambers will be made and be tested until the September of 2023

Figure 15. Photon mask for photon beam exit

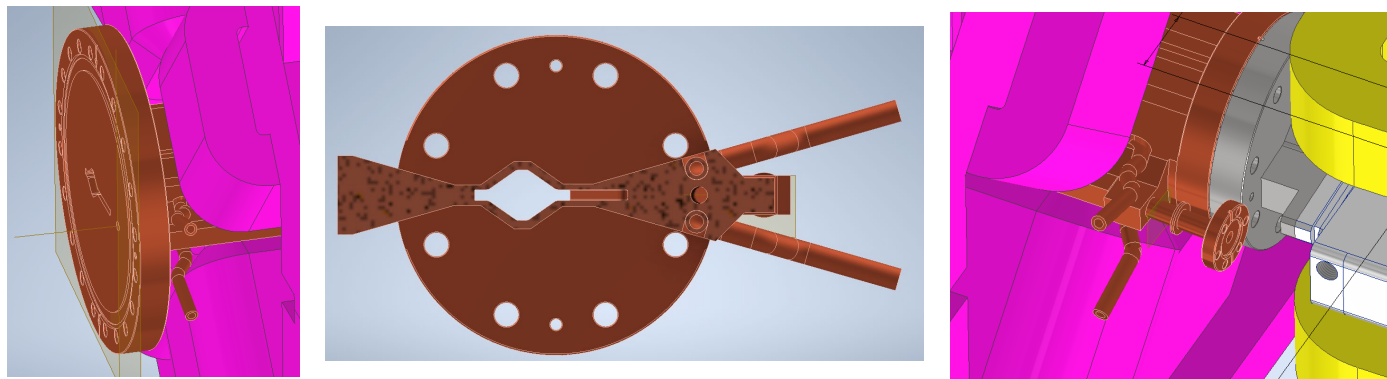
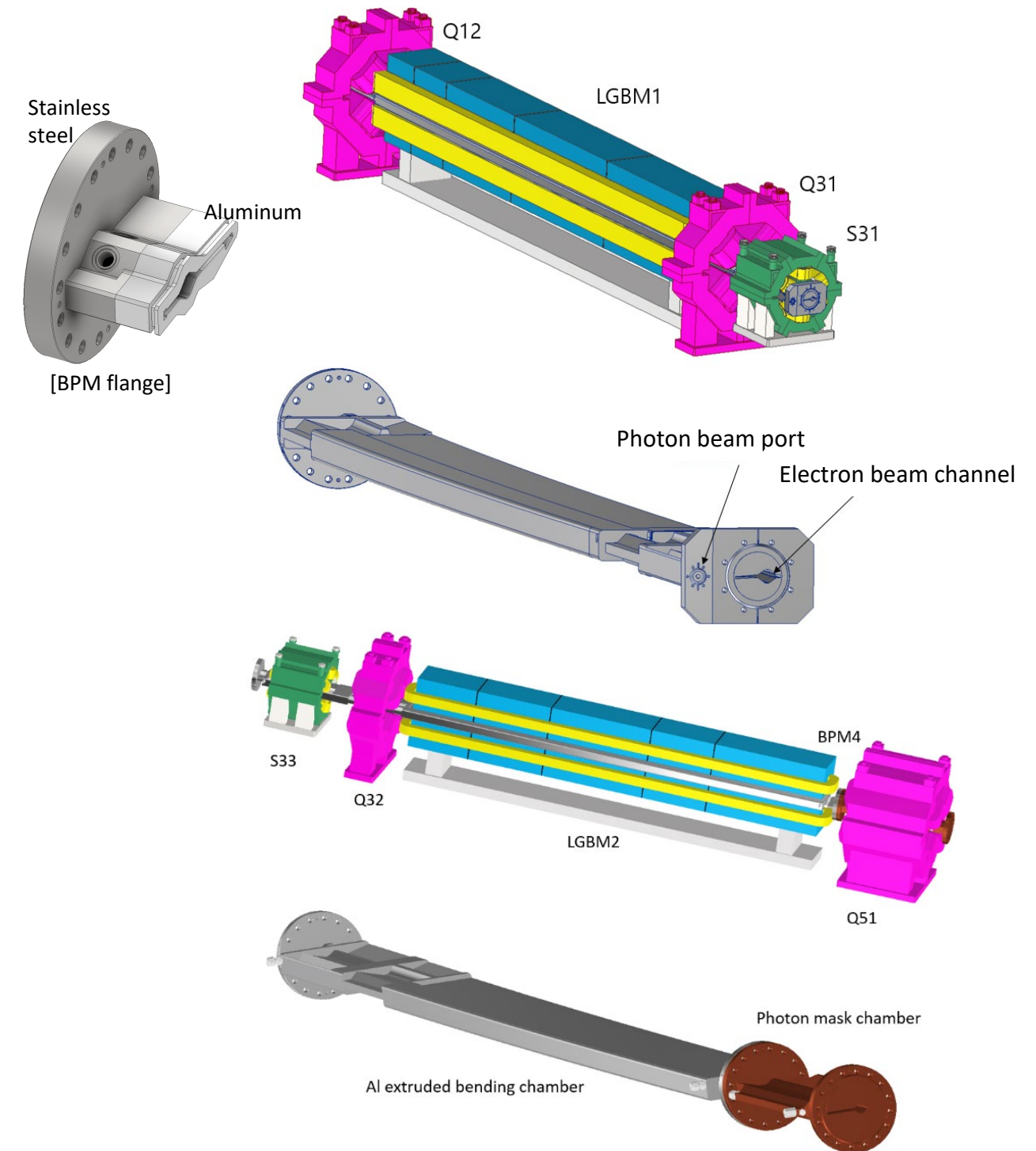


Figure 16. 3D modeling for fabrication of prototype chambers



Booster vacuum chamber

❖ Main features

- Beam chamber cross section is elliptical shape (11 mm (H) x 6 mm (V)).
- Two RF-bellows are used for installation and to reduce stress.
- Sputter ion pumps (60 l/s) are installed at every 5 m along the booster ring. → average pressure of 1.4×10^{-8} mbar
- Pressure of the booster ring is read from controllers of the sputter ion pump
- The clearance between the vacuum chamber and the magnets is larger than 1 mm.

Figure 16. Layout of a booster ring sector

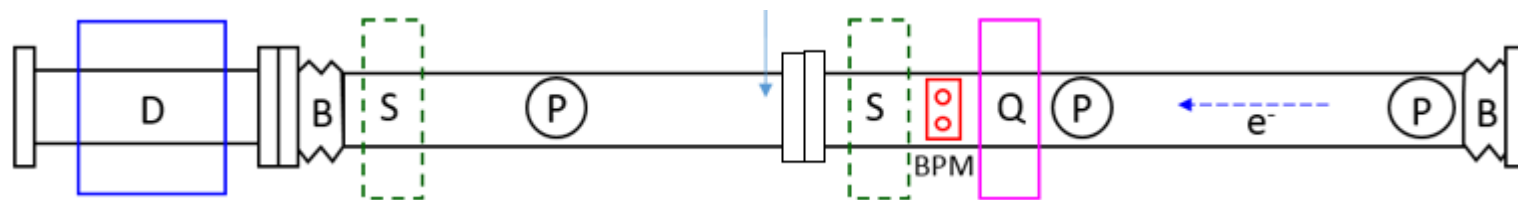
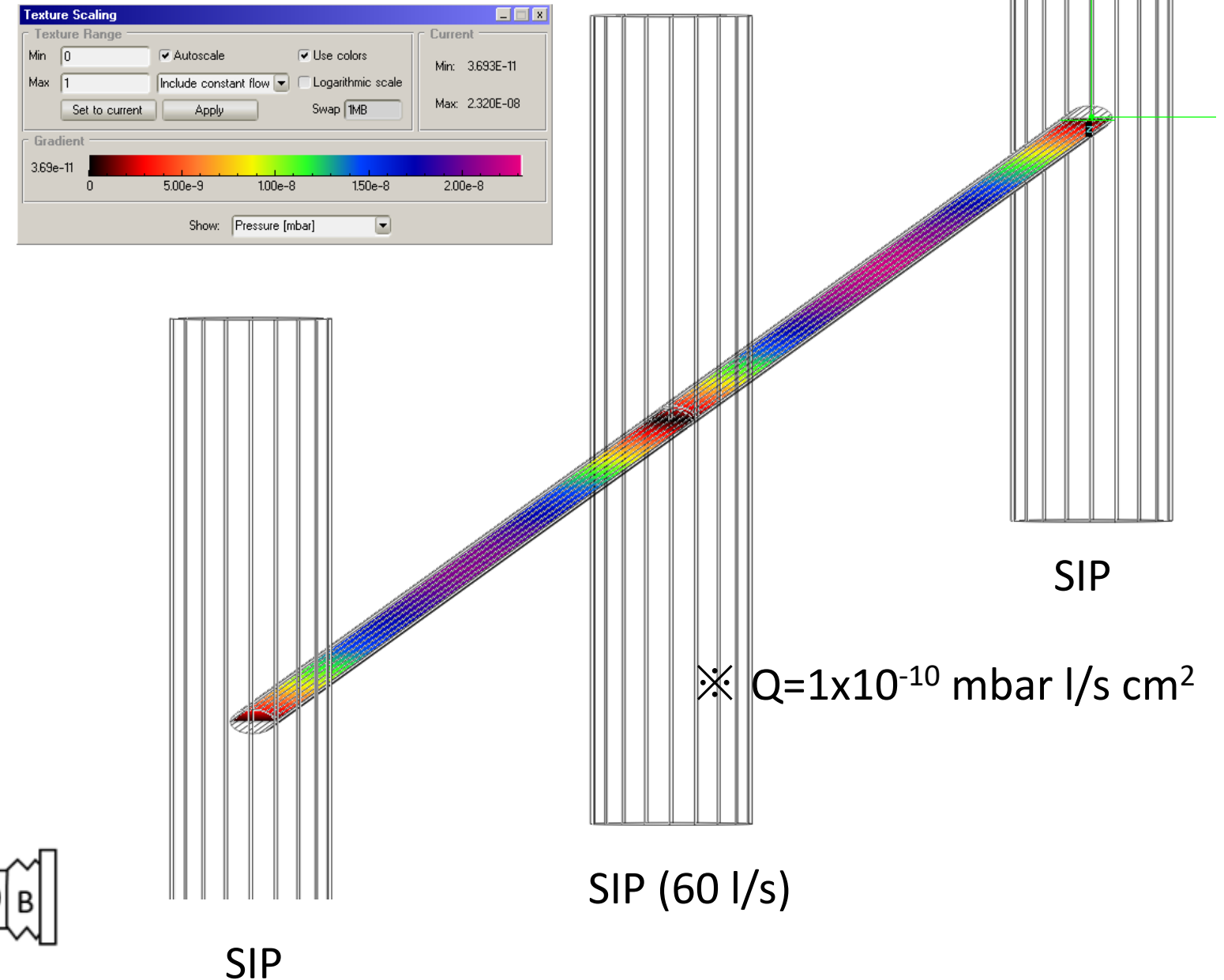


Figure 17. Pressure distribution of the booster ring chamber

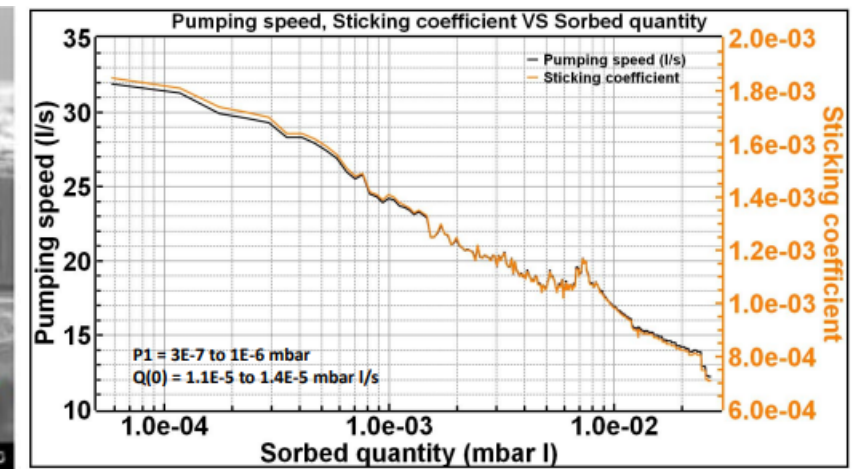
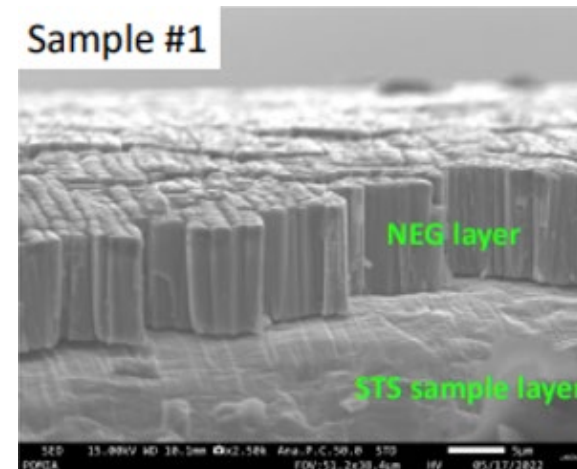
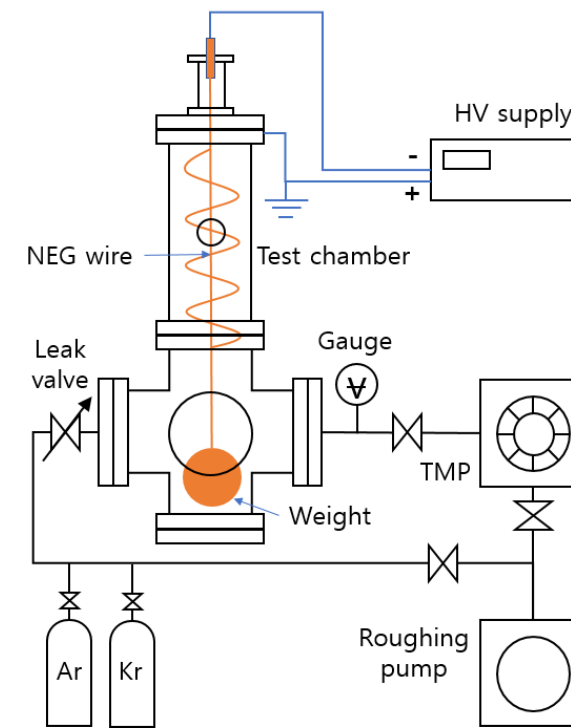


R&D

❖ NEG coated chamber

- NEG coating by DC discharge (no solenoid) in relatively high pressure ($\sim 10^{-2}$ mbar)
- Coated NEG layer on stainless steel shows columnar structure (higher pumping speed)
- Sticking coefficient of a sample chamber is measured to be 1.8×10^{-3}
- NEG coating of $\Phi 20$ mm aluminum chamber will be tested
- More studies for good uniformity and adhesion performance will be done until the end of 2023

Figure 18. NEG coating facility in PAL

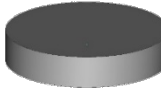

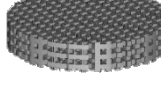
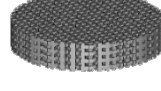


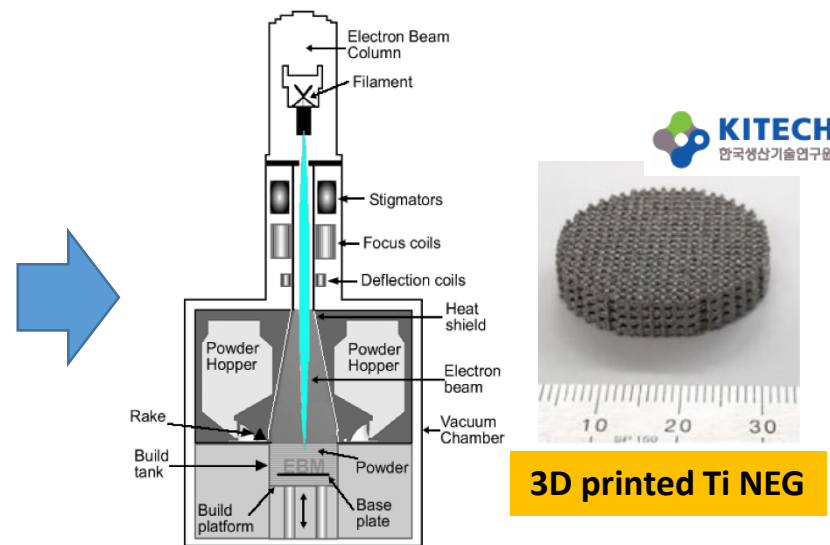
R&D

❖ NEG coated chamber

- Mesh structure design for maximum specific surface area
- Fabrication of Ti getter using 3D printer with titanium powder in vacuum environment (Electron Beam Melting in vacuum → high purity Ti)
- Pumping speed of one 3D printed Ti getter is measured to be 0.6 l/s, which is as much as 60% that of the conventional NEG
- Alloy (Ti, Zr, V, Al,...) powders are necessary to increase the pumping speed and to lower the activation temperature

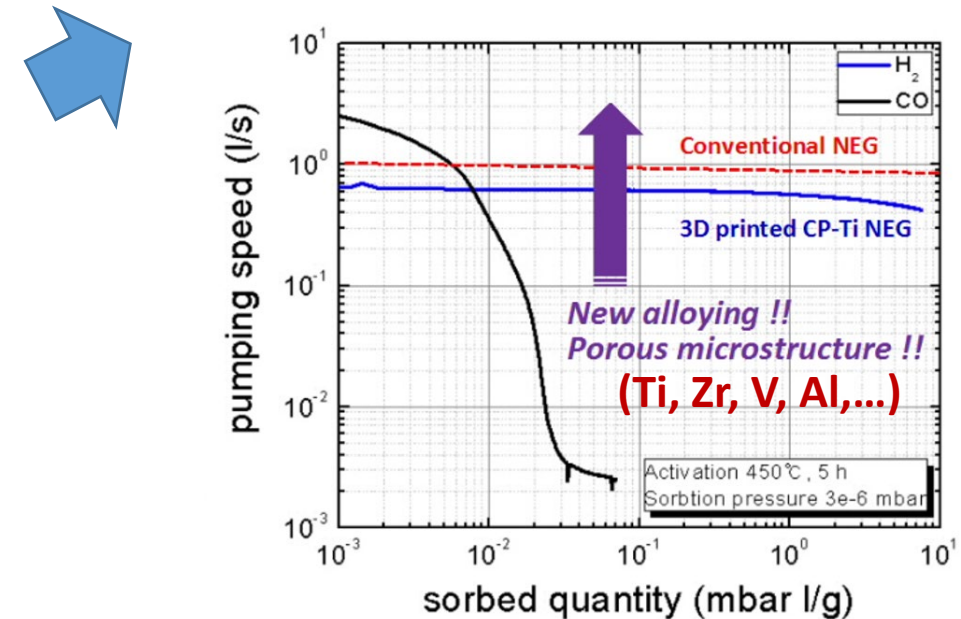
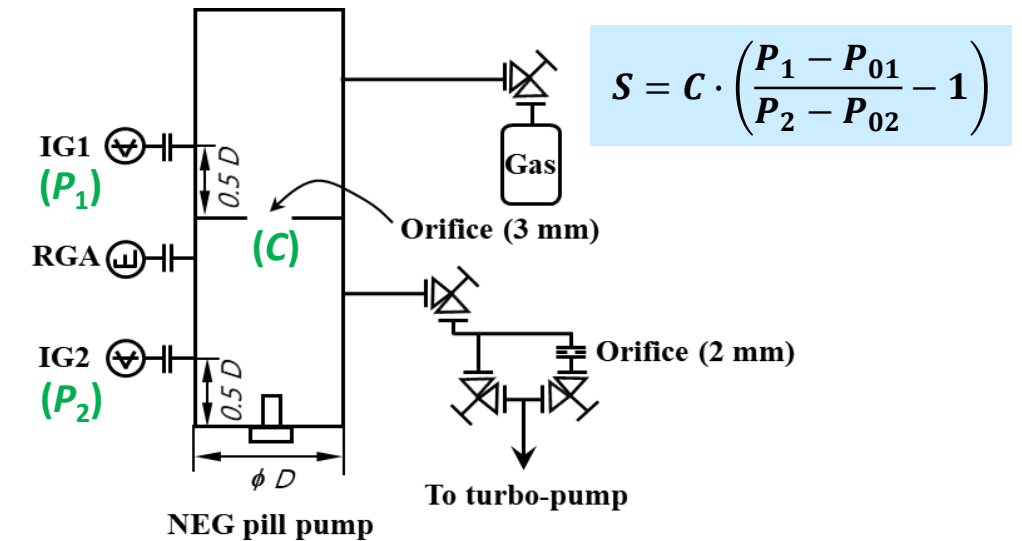
Figure 18. Design of 3D printed getter and fabrication with EBM

Sample	3D CAD design	Diameter (mm)	Height (mm)	Area (mm ²)	Relative Area (%)
Bulk		30	6	1978	100
C2		30	6	4859	246
C3		30	6	6974	353
C4		30	6	9094	460



Electron Beam Melting
[image from MPI.com]

Figure 19. Pumping performance of the 3D printed getter



Summary

❖ Design concept of SR vacuum chamber

- Distributed pumping with pill-type getters and distributed photon absorption with inclined chamber wall
- Chamber materials:
 - Extruded Al chambers (A6063-T6) with cooling channels for bending magnets
 - CuCrZr (C18150) alloy for photon mask and photon beam exit
 - Stainless steel-Aluminum bi-metal chamber for BPMs and flanges

❖ Fabrication of prototype chambers

- 3D modeling of 4 LGBM chambers finished
- Fabrication procedure by local companies has been checked (no problem)
 - ✓ Al chamber extrusion → bending → machining → TiC coating → welding
- Prototype of SR chambers will be made and be tested until the September of 2023

❖ Finalization of vacuum system design

- Design iteration between beam-magnet-vacuum until the end of 2022
- Technical design report by September of 2023

An aerial architectural rendering of a large, circular building complex. The main structure is a wide, multi-story ring with a blue-tinted, ribbed facade. Inside the ring is a central courtyard with a smaller building and greenery. The entire complex is surrounded by lush green trees and a road with cars. In the background, other campus buildings and a misty landscape are visible.

Thank you!

Taekyun Ha (PAL)
E-mail: hatae@postech.ac.kr